

Scalable Transfer Evolutionary Optimization: Coping with Big Task Instances

Mojtaba Shakeri, Erfan Miah, Abhishek Gupta, and Yew-Soon Ong, *Fellow, IEEE*

Abstract—In today’s digital world, we are confronted with an explosion of data and models produced and manipulated by numerous large-scale IoT/cloud-based applications. Under such settings, existing transfer evolutionary optimization frameworks grapple with satisfying two important quality attributes, namely *scalability* against a growing number of source tasks and *online learning agility* against sparsity of relevant sources to the target task of interest. Satisfying these attributes shall facilitate practical deployment of transfer optimization to big source instances as well as simultaneously curbing the threat of *negative transfer*. While applications of existing algorithms are limited to tens of source tasks, in this paper, we take a quantum leap forward in enabling two orders of magnitude scale-up in the number of tasks; i.e., we efficiently handle scenarios with up to thousands of source problem instances. We devise a novel transfer evolutionary optimization framework comprising two co-evolving species for joint evolutions in the space of source knowledge and in the search space of solutions to the target problem. In particular, co-evolution enables the learned knowledge to be orchestrated on the fly, expediting convergence in the target optimization task. We have conducted an extensive series of experiments across a set of practically motivated discrete and continuous optimization examples comprising a large number of source problem instances, of which only a small fraction show source-target relatedness. The experimental results strongly validate the efficacy of our proposed framework with two salient features of scalability and online learning agility.

Index Terms—Big task instances, scalability, transfer evolutionary optimization, negative transfer.

I. INTRODUCTION

There have been sustained attempts at designing algorithms that are able to automatically transfer and reuse learned knowledge across datasets, problems, and domains. The main objective is to promote the *reproducibility* and *generalizability* of intelligent systems in a way that performance efficacy is not only restricted to an individual (narrow) task, but can also be reproduced in other *related* tasks by sharing common *computationally encoded knowledge priors* [1]. *Transfer evolutionary optimization* is one such promising computational paradigm

This work was supported by the A*STAR Cyber-Physical Production System (CPPS) – Towards Contextual and Intelligent Response Research Program, under the RIE2020 IAF-PP Grant A19C1a0018, and Model Factory@SIMTech. (*Corresponding author: Mojtaba Shakeri.*)

M. Shakeri is with Singapore Institute of Manufacturing Technology, Singapore 138634 (e-mail: Mojtaba_Shakeri@simtech.a-star.edu.sg).

E. Miah is with Department of Computing Science, Faculty of Science, University of Alberta, Canada T6G 2E8 (e-mail: miah@ualberta.ca).

A. Gupta is with Singapore Institute of Manufacturing Technology, Singapore 138634 (abhishek_gupta@simtech.a-star.edu.sg).

Y.-S. Ong is with the Data Science and Artificial Intelligence Research Center, School of Computer Science and Engineering, Nanyang Technological University, Singapore 639798, and also with Agency for Science, Technology and Research, Singapore 138632 (e-mail: asysong@ntu.edu.sg).

that enables knowledge transfer in evolutionary optimization via reuse of priors drawn from previously tackled *source* tasks to solve a new *target* task of interest [2].

Reusing knowledge priors from past problem-solving experiences is also known as *sequential transfer* in the related literature [2]. There have been a growing number of successful examples of sequential transfer in areas such as neuro-evolution [3], multi-objective continuous optimization [4], [5], [6], combinatorial optimization [7], [8], [9], [10], dynamic optimization [11], [12], [13], and learning classifier systems [14], [15], [16] with real-world applications from the composites manufacturing industry [5], engineering design [4], [6], [17], last-mile logistics [18], automated machine learning [19], [20], reinforcement learning [21], to name a few.

Generally, there are two common modes for reusing priors in sequential transfer. One is the *exact storage* and reuse of past solutions (either directly [22], [23], [24] or after passing through a mapping function [5], [25]) for subsequent injection into the search space of the target problem. The other is *model-based* transfer where reuse of priors has recently been realized by sampling from probabilistic models of elite candidate solutions drawn from previously solved optimization tasks [26], [27]. Irrespective of which approach is being applied, the challenge is to *efficiently* curb the threat of *negative transfer* when there are *big* source task instances at hand and *many* are not relevant to the target problem. Measuring inter-task similarity, however, requires utilization of problem-specific data that may not be a priori known before the onset of the search, particularly in black-box evolutionary optimization settings which is the focus of this paper. This promoted *online source-target similarity learning* as an effective strategy to mitigate the risks of negative transfer on the fly during the course of the evolutionary optimization [6], [27], [28]. In [6], Zhang *et al.* introduced a multi-source selective transfer framework where inter-task similarity is captured by measuring the Wasserstein distance of the respective source and target search probabilistic models. The final source population is then formed by applying heuristic rules based on the max and variance of similarities across different sources, and, through a mapping function, injects the candidate solutions into a GA-style algorithm. The work utilized Feng *et al.*’s single layer denoising autoencoder [5], [29] as the mapping function to connect source and target populations in continuous search spaces. Their approach, however, requires similarity computations and comparisons at every generation of the evolution to effectively mandate the process of transfer. This incurs significant computational cost when the number of sources starts to grow; see complexity analysis in Section II-B.

The threat of negative transfer was also tackled by Da *et al.* [27]. They developed an adaptive model-based transfer evolutionary algorithm (AMTEA) in which the measure of source-target similarity is defined as the extent of overlap between the optimized source and target search distributions captured via stacked density estimation of the target population. The AMTEA, however, requires a learning algorithm to be nested within the target evolutionary search to reveal latent source-target similarities during the course of the search. This impedes the approach from *scaling* efficiently when large number of source probabilistic models are to be stacked with the target model. Shakeri *et al.* [28] addressed the scaling burden of the AMTEA by incorporating a source selection mechanism based on the theory of multi-armed bandits (MAB) to allow only one source to be stacked with the target each time knowledge transfer is launched. In spite of the fact that MAB is theoretically capable to converge to an optimal strategy (to exploit knowledge from most related sources), the algorithm does not empirically assure that the closest sources to the target will eventually be learned at convergence amid thousands of different source instances. The uniformly random selection of just a single source at initial stages of the MAB often prevents the algorithm from *quickly identifying* the most relevant source(s), especially when the proportion of related sources is small.

With these observations in mind, this paper aims at tackling two critical shortcomings of today’s transfer evolutionary optimization frameworks when deployed to big source task instances that have been produced and manipulated by numerous large-scale IoT/cloud-based applications. The shortcomings are namely lack of *scalability* when faced with a growing bulk of source instances and lack of *online learning agility* against sparsity of relevant sources to the target task of interest. While applications of existing algorithms are limited to tens of source tasks, in this paper, we take a quantum leap forward in enabling two orders of magnitude scale-up in the number of tasks by handling scenarios with up to thousands of source problem instances. We devise a *scalable transfer evolutionary optimization framework*, sTrEvo in short, comprising two co-evolving species for joint evolutions in the space of source knowledge and in the search space of solutions to the target problem. The proposed co-evolutionary transfer mechanism enables the learned knowledge to be rapidly orchestrated on the fly by applying a *two-membered evolution strategy*, i.e., (1+1)-(ES), with a mutation function that can adjust the level of transfer based on the relatedness of sources to the target. The key contribution of this work can thus be summarized as follows.

- 1) We establish a scalable transfer evolutionary optimization framework with two salient features of scalability and online learning agility through co-evolution in the knowledge and target search spaces.
- 2) We incorporate a novel mutation mechanism in the (1+1)-ES based knowledge extraction algorithm that enables rapid and effective utilization of relevant source problem instances up to two orders of magnitude larger in number than those encountered in existing works.

- 3) We empirically verify the efficacy of the algorithm through an extensive and rigorous experimental study across a set of practically motivated discrete and continuous optimization examples.

The rest of the paper is organized as follows. Section II contains preliminaries on model-based transfer evolutionary optimization and conducts a complexity comparison for some of the state-of-the-art algorithms. Section III presents our proposed sTrEvo with its underlying (1+1)-ES based knowledge extraction module. In Section IV, extensive experiments supplemented with rigorous analyses are conducted for assessing the scalability of sTrEvo across three case studies ranging from discrete to continuous search spaces. Finally, in Section V, we conclude the paper and highlight potential future research directions.

II. PRELIMINARIES

A. Basics of Model-Based Transfer

The probabilistic model-based expression of a typical optimization problem \mathcal{T} with a maximization function $f(\mathbf{x})$ (we adopt $-f(\mathbf{x})$ if the underlying optimization problem is one of minimization) over a search space \mathcal{X} is mathematically formulated as,

$$\max_{p(\mathbf{x})} \int_{\mathcal{X}} f(\mathbf{x}) \cdot p(\mathbf{x}) \cdot d\mathbf{x}, \quad (1)$$

where, $p(\mathbf{x})$ is the probability search distribution of candidate solutions in \mathcal{X} . Given a global optimum fitness value f^* , a distribution $p^*(\mathbf{x})$ generating high-quality (near optimal) solutions of \mathcal{T} should satisfy the following,

$$\int_{\mathcal{X}} f(\mathbf{x}) \cdot p^*(\mathbf{x}) \cdot d\mathbf{x} \geq f^* - \varepsilon, \quad (2)$$

here, ε represents a small positive convergence threshold. Note that in the case we let ε be 0, $p^*(\mathbf{x})$ could then become a degenerate distribution that collapses to just a single point; this is not what we want.

In the sequential transfer optimization setting, when the objective is to optimize *target* task \mathcal{T}_T , we assume that there are $T - 1$ *source* tasks $\mathcal{T}_1, \dots, \mathcal{T}_{T-1}$ with maximization functions $f_1(\mathbf{x}), \dots, f_{T-1}(\mathbf{x})$ whose search distributions are already optimized over a unified search space \mathcal{X} that encodes solutions corresponding to all T tasks. A complete description of unified search spaces can be found in [3]; details are left out herein for the sake of brevity. Under this setting, the evolutionary transfer optimization of the target problem from the viewpoint of probabilistic model-based search is described mathematically as [3],

$$\begin{aligned} & \max_{w_1, \dots, w_{T-1}, w_T, p_T(\mathbf{x})} \int_{\mathcal{X}} f_T(\mathbf{x}) \cdot \left[\sum_{s=1}^{T-1} w_s \cdot p_s^*(\mathbf{x}) + w_T \cdot p_T(\mathbf{x}) \right] \cdot d\mathbf{x} \\ & \text{such that } \sum_{i=1}^T w_i = 1 \text{ and } w_i \geq 0, \forall i \in \{1, \dots, T-1, T\}. \end{aligned} \quad (3)$$

In this formulation, w_1, \dots, w_{T-1}, w_T are referred to as *transfer coefficients* in the probabilistic mixture model

$[\sum_{s=1}^{T-1} w_s \cdot p_s^*(\mathbf{x}) + w_T \cdot p_T(\mathbf{x})]$, and determine the extent of knowledge transfer from each source to the target. The mixture model is trained to capture the true underlying distribution of the target population, from which candidate solutions are sampled to adaptively bias the target search. A proper adjustment of the coefficients is challenging nonetheless as there is assumed to be no prior knowledge on the optimal search distribution $p_T^*(\mathbf{x})$ of the target problem to help identify related and unrelated sources offline. The consequences of improper assignments are twofold. On one hand, designating an unreasonably high transfer coefficient to an unrelated source model will result in injecting poor solutions into the search space of the target that may significantly impede the target search performance. On the other hand, the inability to assign an adequately high value to a relevant source model suppresses the transfer of useful solutions to improve optimization efficiency in the target task. The challenge is more severe in black box optimization. Due to the absence of an algebraic model of the system to be optimized in such settings, we can only rely on online data generated during the course of target optimization to discover inter-task similarities. It is thus crucial for a transfer optimization algorithm to be able to accurately orchestrate the mixture transfer coefficients of (3) based on the data generated during the target optimization search.

B. State-of-the-Art Transfer EAs

It can be inferred from (3) that the optimization of the target probabilistic model as well as adjustment of the mixture transfer coefficients are two intertwined components of the online model-based transfer optimization. The adaptive model-based transfer EA framework (AMTEA), as proposed in [27], captures the latter via stacked density estimation of the target population [30]. At any generation of the target EA where knowledge transfer is launched, a mixture model comprising a linear composition of T available probabilistic models is learned from n solutions (of dimensionality d) of the current generation by finding the optimal configuration of the transfer coefficients corresponding to each model. The learning process is carried out by applying the classical *expectation-maximization* (EM) algorithm [31], which, in the context of stacked density estimation, entails the construction of an $n \times T$ probability matrix to capture the likelihood of each solution corresponding to all the T probabilistic models [27]. Overall, this requires $\mathcal{O}(dnT)$ computational steps for a variable-wise factored distribution model, in addition to the complexity of executing the EM algorithm itself. The cost for learning *optimal* transfer coefficient values is that AMTEA does not scale efficiently when the number of sources grows to hundreds and beyond.

The lack of scalability of the AMTEA was tackled in [28] via a source selection algorithm that runs in $\mathcal{O}(T)$ to choose only one source model at a time for stacked density estimation. This reduces the computational steps required for constructing the probability matrix to $\mathcal{O}(dn)$, which is a significant speedup when there are thousands of source models available. The selection strategy is formulated based on a popular variant of the multi-armed bandit problem, known as the adversarial MAB

[32] which can be solved to optimality using the *Exponential-weight algorithm for Exploration and Exploitation* (EXP3) [33]. In this setting, each source corresponds to an arm of a bandit whose reward, when chosen (pulled), is proportional to its level of similarity to the target. A source model which can generate fitter individuals, as evaluated by the target objective function, receives a higher reward measure and is more likely to be chosen in future generations. However, as was noted in Section I, the uniformly random selection of just a single source at initial stages of the MAB often hinders the algorithm from rapidly identifying the most relevant source(s), especially when related sources are sparse. An extensive series of experiments and analyses to evaluate the above algorithms and claims will be carried out in Section IV. We denote the MAB-enabled AMTEA developed in [28] as MAB-AMTEA for the remainder of the paper.

There is another class of sequential transfer methods that builds a single layer mapping function to inject solutions of past search experiences into the current target population while the optimization search progresses [5]. The mapping function is built each time knowledge transfer occurs. Given two solution populations (one pertaining to a previously solved source task and the other to the target problem) both of which consist of n solutions of d dimensions, a basic implementation requires $\mathcal{O}(nd^2 + d^3)$ computational steps to construct the mapping function. (Detailed computational analyses are not presented here for the sake of brevity.) The above process, however, is not scalable when the number of sources is large (i.e., $T \gg 1$), as it needs to be repeated per source to build the corresponding mapping function; this makes the complexity scale as $\mathcal{O}(T(nd^2 + d^3))$. In addition, memory consumption is another resource bottleneck as it is required to archive the solutions data of all source instances for all generations, which can quickly become intractable. Although the challenge of multiple sources was addressed in [6] by proposing a source selection mechanism (at additional expense of $\mathcal{O}(dnT + T\sqrt{T})$) to form a single population to construct the mapping function, the memory consumption bottleneck remains. In contrast, in the probabilistic model-based sequential transfer methods, we only need to store the learned search distribution models, comprising only few distribution parameters. Finally, note that the existing single layer autoencoder method only applies to continuous search spaces.

III. SCALABLE TRANSFER EVOLUTIONARY OPTIMIZATION

In this section, we devise our novel scalable transfer evolutionary optimization framework (sTrEvo) which comprises two co-evolving species for joint evolutions in the space of source knowledge and in the search space of solutions to the target problem. The proposed co-evolutionary transfer mechanism enables rapid and effective utilization of the learned knowledge amongst thousands of source problem instances by applying a two-membered evolution strategy, i.e., (1+1)-(ES), with a novel mutation function capable of adjusting the level of transfer in accordance with the relatedness of sources to the target. In this work, the species to evolve the solutions to the target problem is just a canonical EA (although any other

preferred algorithm can be used). In the following, we will describe the components of the sTrEvo in detail.

A. Source Knowledge Evolution in STrEvo

The core component of the sTrEvo is the knowledge extraction module which is based on the (1+1)-ES. In the (1+1)-ES, one solution is evolved per generation by being mutated. The fitness of the two solutions (i.e., the parent and its offspring) is compared and the best of the two is chosen as the individual for the next generation. In our setting, the *chromosome* is encoded as the transfer coefficients in the mixture model and the *fitness* is defined as the mean fitness of candidate solutions generated from the corresponding mixture model and evaluated by the objective function of the target problem. The algorithm evolves for one generation every time it is launched by the target EA for knowledge transfer, the frequency of which is determined by a *transfer interval* (denoted by Δ generations as specified in Procedure 2).

In the standard (1+1)-ES, the parent is mutated according to a mutation radius, a random variable following a normal distribution. In this paper, however, we propose a different mutation mechanism according to the characteristics of the transfer optimization paradigm as formulated in (3). Given that $\int_{\mathcal{X}} f(\mathbf{x}) \cdot p(\mathbf{x}) \cdot d\mathbf{x}$ indicates the expected objective value of a search distribution model $p(\mathbf{x})$ against an objective function $f(\mathbf{x})$ over a search space \mathcal{X} , we rephrase the formulation in (3) as follows,

$$\begin{aligned} \max_{w_1, \dots, w_{T-1}, w_T, p_T(\mathbf{x})} & w_1 \cdot E_{\mathbf{x} \sim p_1^*(\mathbf{x})} [f_T(\mathbf{x})] + \dots \\ & + w_{T-1} \cdot E_{\mathbf{x} \sim p_{T-1}^*(\mathbf{x})} [f_T(\mathbf{x})] \\ & + w_T \cdot E_{\mathbf{x} \sim p_T(\mathbf{x})} [f_T(\mathbf{x})], \end{aligned} \quad (4)$$

where $E_{\mathbf{x} \sim p_s^*(\mathbf{x})} [f_T(\mathbf{x})]$ is the expected fitness of an optimized source probabilistic model $p_s^*(\mathbf{x})$ relative to the target objective function $f_T(\mathbf{x})$. Also note that $\sum_{i=1}^T w_i = 1$ and $w_i \geq 0$, $\forall i \in \{1, \dots, T\}$.

As the overall objective in (4) is formulated as that of maximization, a higher expected value for each model should be reinforced with a higher corresponding transfer coefficient. This forms the basis for our novel mutation method as a means of guiding the evolution toward maximizing positive transfer by giving higher weights to related sources as well as suppressing negative transfer by neutralizing weights to unrelated ones. We implement this by defining a mutation vector of size T such that the first $T-1$ elements correspond to the source models and the last refers to the target. Each entry in the mutation vector estimates the expected fitness of its corresponding probabilistic model. This is done by recording the up-to-date average fitness of candidate solutions that have been generated from the model and evaluated by the target objective function during the course of knowledge transfer. Note that as the knowledge extraction progresses, the samples generated from the models accumulate accordingly, leading to have more accurate estimations of their corresponding expected fitness. After mutation is carried out per generation, a new mixture model is formed from which a sample population

is generated for knowledge transfer. For clarity, we present the details of the (1+1)-ES based knowledge extraction module in pseudocode in Procedure 1 for the case of a maximization problem.

Procedure 1: (1+1)-ES Based Knowledge Extraction

Input: Optimized source models $p_1^*(\mathbf{x}), \dots, p_{T-1}^*(\mathbf{x})$, scaling factor ζ , learning rate η , target task \mathcal{T}_T , transfer counter t , target population P_t , mean target fitness $\bar{f}_{T,t}$;

- 1 **if** $t == 0$ **then**
- 2 Initialize transfer coefficients $w_t[1 : T]$ with $1/T$;
- 3 Initialize mutation vector $\pi[1 : T]$ with zeroes;
- 4 Build target model $p_{T,t}(\mathbf{x})$ using P_t ;
- 5 Form mixture model M_t from $p_1^*(\mathbf{x}), \dots, p_{T-1}^*(\mathbf{x})$, $p_{T,t}(\mathbf{x})$ and $w_t[1 : T]$;
- 6 Generate candidate transfer solutions X_t from M_t using the Monte Carlo sampling method;
- 7 Evaluate solutions in X_t using target objective function $f_T(\mathbf{x})$ and record the mean fitness as \bar{f}_t ;
- 8 **else**
- 9 **for** $s = 1$ **to** $T - 1$ **do**
- 10 | $\pi[s] \leftarrow$ average fitness of candidate solutions in $\bigcup_{i=1}^{t-1} X_i$ that have been sampled from $p_s^*(\mathbf{x})$;
- 11 $\pi[T] \leftarrow \bar{f}_{T,t}$;
- 12 **for** $i = 1$ **to** T **do**
- 13 | $\pi'[i] \leftarrow (\pi[i] / \max(\pi[1 : T])) \times \zeta$;
- 14 **for** $i = 1$ **to** T **do**
- 15 | $\pi''[i] \leftarrow e^{\pi'[i]} / \sum_{j=1}^T e^{\pi'[j]}$;
- 16 | $w'[i] \leftarrow (1 - \eta) \times w_{t-1}[i] + \eta \times \pi''[i]$;
- 17 **for** $i \leftarrow 1$ **to** T **do**
- 18 | **if** $w'[i] \leq \epsilon$ **then** Neutralize $w'[i]$ by 0 ;
- 19 **for** $i \leftarrow 1$ **to** T **do**
- 20 | $w''[i] \leftarrow w'[i] / \sum_{j=1}^T w'[j]$;
- 21 Build target model $p_{T,t}(\mathbf{x})$ using P_t ;
- 22 Form mixture model M_t from $p_1^*(\mathbf{x}), \dots, p_{T-1}^*(\mathbf{x})$, $p_{T,t}(\mathbf{x})$ and $w''[1 : T]$;
- 23 Generate candidate transfer solutions X_t from M_t using the Monte Carlo sampling method;
- 24 Evaluate solutions in X_t using target objective function $f_T(\mathbf{x})$ and record the mean fitness as \bar{f}' ;
- 25 **if** $\bar{f}' \geq \bar{f}_{t-1}$ **then**
- 26 | $w_t[1 : T] \leftarrow w''[1 : T]$;
- 27 | $\bar{f}_t \leftarrow \bar{f}'$;
- 28 **else**
- 29 | $w_t[1 : T] \leftarrow w_{t-1}[1 : T]$;
- 30 | $\bar{f}_t \leftarrow \bar{f}_{t-1}$;
- 31 **return** X_t

As already stated, Procedure 1 is called by the target EA each time knowledge transfer occurs. This is traced by a *transfer counter* (t) which is input to the procedure and indicates the current generation of knowledge extraction. Accordingly, $t = 0$ represents the initialization phase (lines 2–7) in which

the initial chromosome is formed by assigning identical values (here, $1/T$) to the transfer coefficients. This implies that each source model, as well as the initial target model, has an equal probability to transfer candidate solutions to the target optimization algorithm. These individuals are evaluated by the target objective function and the mean fitness is recorded as the fitness of the initial chromosome.

For the case of $t > 0$, the knowledge extraction proceeds with updating the mutation vector (lines 9–11). As already discussed, each entry in the mutation vector estimates the expected fitness of its corresponding model against the target problem and is measured by taking the average fitness of candidate solutions that have been sampled from that model. The average fitness to a source model is updated each time a new solution is added. This is done incrementally in a constant time without the need to keep the previous solutions in memory. Assume that the mutation entry $\pi[s]$, corresponding to the source model $p_s^*(\mathbf{x})$, holds the average fitness over the first $i - 1$ solutions; the updated average after adding the i th candidate solution \mathbf{x}_i sampled from $p_s^*(\mathbf{x})$ is calculated as follows,

$$\pi[s] \leftarrow \pi[s] + \frac{f_T(\mathbf{x}_i) - \pi[s]}{i}. \quad (5)$$

Note that unlike the source probabilistic models which remain fixed during the target optimization, the target model is non-stationary and is rebuilt each time knowledge transfer occurs. This hinders the incremental update of the average fitness, as done for the source models, from being applied to the target. Alternatively, since the solutions to build the target model are evaluated in the target evolutionary search procedure before being passed to the knowledge extraction module, it is possible to compute their mean fitness in the same procedure and pass it along with the target population.

Thereafter, a two-stage transformation is carried out on the mutation vector to help online source-target similarity to be captured more rapidly and effectively. This is realized by applying the *maximum absolute scaling* and *softmax* functions, respectively (lines 13 and 15). The output from the former is a real-valued vector between zero and one where the entries have been scaled relative to the value of the maximum element. We nevertheless observed that effective exploitation from more related sources requires a more meaningful distinction amongst the values. Accordingly, the resultant mutation vector is scaled to a wider range by being multiplied by a so-called *scaling factor* (ζ) defined as a hyper-parameter (line 13). Tuning the parameter with higher values enforces more exploitation whereas lower values make room for more exploration across the source models. Eventually, mutation is carried out in Line 16 to generate the offspring from the parent chromosome and mutation vector. A *learning rate* (η), also defined as a hyper-parameter in the interval $[0, 1]$, is applied to delay early convergence to those sources that receive higher probabilities during mutation, allowing exploring sources with lower probabilities. The lower is the value, the more intense is the exploration.

The updated transfer coefficients in the offspring form a new mixture model that should be used to generate new

candidate solutions. This, however, is deferred until a neutralization function is carried out on each element of the offspring (line 18). If the value is below a very small positive threshold, then the entry (which entails the transfer coefficient to a source model) is neutralized to zero, meaning that the corresponding source is identified unrelated and hence, should not be sampled for the remaining generations. The rationale behind such adjustment lies in the Monte Carlo sampling method being used, as it ensures that at least one sample is generated from every source model whose corresponding transfer coefficient is positive (no matter how close the value is to zero). Consequently, in situations where the number of sources is significantly greater than the population size, there could be no chance for those models with a slightly larger transfer coefficient to have their sample(s) chosen as candidate solutions for transfer. In this regard, neutralizing the sources with extremely low transfer coefficients is deemed an effective strategy to remedy this undesirable property.

The last part of the code, i.e., lines 25–30, deals with evolution in which the parent is replaced with the offspring if its fitness is not better than that of the offspring. Lastly, note that irrespective of whether or not the offspring replaces its parent, the candidate solutions generated from its corresponding mixture model are always returned for the utilization of the target evolutionary search. This is because there might be a handful of high-quality solutions (among a majority of low-quality ones) that are able to improve optimization efficiency in the target problem.

B. Target Solutions Evolution in STrEvo

Our proposed (1+1)-ES can be incorporated as a nested module within any canonical or state-of-the-art EA to optimize the target task. Procedure 2 presents such integration for a canonical GA (CGA) in pseudocode. In this setting, the transfer interval Δ is defined to specify the frequency of calling the knowledge extraction module in number of generations. Upon the call, the (1+1)-ES advances for one generation.

Procedure 2: Pseudocode of sTrEvo for a CGA

Input: Target task \mathcal{T}_T , transfer interval Δ ;
Output: Optimized target probabilistic model;

- 1 Configure initial population P_0 at random;
- 2 Evaluate solutions in P_0 ;
- 3 $i \leftarrow 0$; /* generation counter */
- 4 $t \leftarrow 0$; /* transfer counter */
- 5 **while** *stopping criteria not satisfied* **do**
- 6 **if** $\text{mod}(i, \Delta) == 0$ **and** $i > 1$ **then**
- 7 $\bar{f}_{T,t} \leftarrow$ mean fitness of solutions in P_i ;
- 8 Call Procedure 1 to form offspring O ;
- 9 $t \leftarrow t + 1$;
- 10 **else**
- 11 Generate offspring O by reproduction of P_i ;
- 12 Evaluate solutions in O ;
- 13 Select next population P_{i+1} from $P_i \cup O$;
- 14 $i \leftarrow i + 1$;

According to the procedure, after the initial population is configured and evaluated (lines 1 and 2), the iterative routine to optimize the target solutions follows two different branches of evolution. Whenever knowledge transfer occurs, the offspring is formed from the candidate solutions returned by the knowledge extraction module (lines 6–9). Otherwise, it is generated by applying the common reproduction operators (line 11). After being evaluated, the offspring is combined with the current population to form the next generation by using a selection mechanism (lines 12 and 13). Note that before the knowledge extraction module is launched at line 8, the mean fitness of solutions in the current population is computed and passed as the input parameter – along with the transfer counter t – to the module (also see Procedure 1). The above steps continue until some stopping criteria are eventually met.

C. Complexity Comparison of sTrEvo

The learning process of the transfer coefficients in the sTrEvo is carried out by the mutation mechanism of the (1+1)-ES. To this end, the T entries in the mutation vector are updated each time a new candidate solution is added from the mixture model. According to (5), this is done in a constant time per added solution, which, overall, requires $\mathcal{O}(n)$ computational steps for n solutions. (Note that computing the mean fitness of the target population, to update the last entry of the mutation vector, also requires $\mathcal{O}(n)$ steps for a population size of n .) Thereafter, the two-stage transformation as well as the generation of the offspring (that encodes the updated transfer coefficients) are carried out in $\mathcal{O}(T)$. Thus, the total complexity of the mutation mechanism becomes $\mathcal{O}(n + T)$. As is clear, the (1+1)-ES, and hence the sTrEvo as a whole, scales much more efficiently than the existing AMTEA with the learning complexity $\mathcal{O}(dnT)$.

IV. EXPERIMENTAL STUDY

In this section, we conduct extensive experiments to assess the efficacy of sTrEvo with regard to *scalability* and *online learning agility*. The assessment is carried out across a set of practically motivated discrete and continuous optimization examples. Following our complexity analysis in Section II-B, note that the single layer autoencoder method proposed in [5] and [6] requires archiving the solutions data of all source instances for all generations, to construct the mapping function whenever knowledge transfer is launched. This entails a significantly large and growing memory cost for evaluation scenarios with 1000 sources and beyond. As a more practically feasible alternative, we compare sTrEvo with state-of-the-art probabilistic model-based transfer methods that only need to store the learned search distribution models, which comprises only few distribution parameters and hence consumes low memory. Our comparative evaluations are accordingly conducted against AMTEA [27] and the MAB-enabled AMTEA (i.e., MAB-AMTEA) [28] algorithms, along with a number of modern solvers without transfer capability. This includes a canonical GA (CGA) enhanced with a local solution repair heuristic for discrete optimization and two powerful variants of the recently proposed *natural evolution strategies* (NESs) [34], namely sNES and xNES, for continuous examples.

A. Experimental Setup

All the compared algorithms were implemented in Python 3.7¹ and run on a 64-bit Intel(R) Core™ i7-7700HQ with 4 cores and 8 logical processors. The OS was Ubuntu 20.04 with 16GB memory. Throughout all experiments, we used an *elitist* selection strategy in the three transfer evolutionary algorithms, i.e., AMTEA, MAB-AMTEA and sTrEvo, as well as the CGA. The (unified) search space representation together with the choice of probabilistic models were determined according to the characteristics of the underlying problem. For discrete optimization, the following general settings were adopted in our compared algorithms:

- 1) Representation: binary coded.
- 2) Population size: 50.
- 3) Maximum function evaluations: 5000.
- 4) Evolutionary operators:
 - a) uniform crossover with probability $\rho_c = 1$,
 - b) bit-flip mutation with probability $\rho_m = 1/d$, where d is the chromosome length.
- 5) Probabilistic model: univariate marginal frequency (factored Bernoulli distribution) [35].

On the other hand, for the chosen set of continuous optimization examples, the following configuration was used:

- 1) Representation: real-valued coded.
- 2) Population size: 50.
- 3) Maximum function evaluations: 5000.
- 4) Evolutionary operators for AMTEA, MAB-AMTEA and sTrEvo:
 - a) simulated binary crossover [36] with $\rho_c = 1$ and distribution index $\eta_c = 10$,
 - b) polynomial mutation [37] with $\rho_m = 1/d$ (d is the chromosome length) and distribution index $\eta_m = 10$.
- 5) Probabilistic model: multivariate Gaussian distribution [38].

For fairness of comparison, we considered identical population size and maximum function evaluations for both sNES and xNES algorithms. The other parameters of the two solvers were configured with default settings from [39]. Note that the above configuration was adopted following the experimental study carried out in [27] for the assessment of the AMTEA approach. With regard to assessing the MAB-AMTEA, there is an egalitarianism factor γ in the EXP3 that was set to 0.1 according to [28].

As there are a few hyper-parameters that need to be tuned for the (1+1)-ES algorithm nested in sTrEvo, preliminary experiments were conducted to identify a proper yet general setting accordingly. The resultant configuration is shown in Table I. Note that ϵ is the threshold value used to neutralize unrelated sources (see Procedure 1) where T is the total number of probabilistic models including the target model. Lastly, we should note that the last setting for the transfer interval also apply to both AMTEA and MAB-AMTEA.

¹The source code is available at <https://github.com/erfanMhi/Transfer-Optimization>.

TABLE I: Hyper-parameter setting for the (1+1)-ES.

Parameter	Setting
Scaling factor (ζ)	100
Learning rate (η)	0.9
Threshold value (ϵ)	$1/T \times 0.01$
Transfer interval (Δ)	2

B. The Discrete 0/1 Knapsack Problem

The knapsack problem (KP) is a well-known NP-hard problem in combinatorial (discrete) optimization and has been studied extensively by the operations research community. There are many variations of the problem with applications in supply chain and logistics optimization, wireless communications and investment decision making, among many others.

The basic version of the problem is the 0/1 KP in which there are d number of items (representing the problem dimensionality), each with a value v_i and a weight w_i , and a knapsack of a finite capacity C . The objective is to find a subset of items such that they can be placed into the knapsack while their total value is maximized. We can describe the problem mathematically as follows,

$$\begin{aligned} & \max \sum_{i=1}^d v_i x_i \\ \text{s.t. } & \sum_{i=1}^d w_i x_i \leq C, \text{ and } x_i \in \{0, 1\}, \end{aligned} \quad (6)$$

here, x_i is a binary decision variable and equals 1 if the i th item is selected and 0, otherwise. It should be noted that solving KP instances using EAs may cause the capacity constraint to be violated for some individuals during the course of evolution. On such occasions, a repair mechanism is invoked to satisfy the constraint in accordance with Dantzig’s greedy approximation algorithm [40].

In this paper, we generate synthetic KP instances with similar characteristics as instructed in [27] and [28]. Depending on the relationships between the w ’s and v ’s, the instances are generated according to *uncorrelated* (un), *weakly correlated* (wc), and *strongly correlated* (sc) categories. The second categorization defines two types of knapsacks based on the number of items that can be selected: a knapsack of a *restrictive capacity* (rc) and one of an *average capacity* (ac). In the former, the allowable number is limited to a small value whereas in the latter, the number could be larger. Having combined the two, we define a $d = 1000$ -D KP configuration in which the target is “KP_uc_ac” and the source instance types are “KP_uc_rc”, “KP_wc_rc”, “KP_sc_rc” and “KP_sc_ac”. Here, the related source type is “KP_sc_ac” implying that a relatively large number of items need to be selected as also must be done for the target.

Two evaluation scenarios were defined to investigate the performance of the sTrEvo with respect to the two important quality attributes, i.e., *scalability* and *online learning agility*. The scenarios are described as follows:

- *Scenario (A)*: where the number of sources is 1000 with 250 instances of the related type and 750 instances

equally distributed among the three unrelated types (relatedness ratio is 0.25).

- *Scenario (B)*: where the number of sources is 1000 with only 40 instances of the related type and 960 instances equally distributed among the three unrelated types (relatedness ratio is 0.04).

A binary CGA was first configured to construct the probabilistic models of all source instances to optimality. We then compared the performance of our proposed sTrEvo with CGA, AMTEA, MAB-AMTEA for both evaluation scenarios. The averaged results obtained over 30 independent runs are shown in Figure 1. With respect to the convergence efficiency, Figures 1a and 1b present the convergence trends of the compared algorithms for Scenario (A) with 250 related sources and Scenario (B) with 40 related sources, respectively. It can be seen from the convergence trends that utilization of related knowledge from previously solved experiences in essence does improve optimization efficiency in the target problem. Such efficiency, however, is more noticeable for sTrEvo. The algorithm acquires a steeper convergence curve than AMTEA and, in particular, MAB-AMTEA in early function evaluations. The reason for such different convergence trends lies in how agile the online learning mechanism of the compared methods is to discern related sources and exploit useful knowledge accordingly. We can therefore conclude that MAB-AMTEA fails to reach that level of agility as opposed to AMTEA and sTrEvo. Put differently, under big source problem instances (here, 1000), effective exploration of sources for identifying and then exploiting the related ones play a determinant role for the sTrEvo in acquiring online learning agility. This is more evident for Scenario (B) in which the proportion of related sources is small. The advantage of such capability (i.e., to achieve convergence in fewer number of function evaluations) would be more significant for case studies where the evaluation of the objective function is very costly.

We also plot the convergence trend of the three compared transfer evolutionary algorithms within the convergence time of sTrEvo as shown in Figures 1c and 1d for Scenarios (A) and (B), respectively. While the MAB-AMTEA is able to converge within this time limit², AMTEA falls much behind the other two and requires a considerably longer time to eventually converge to optimality. The above observations indicate that neither AMTEA nor MAB-AMTEA are able to ensure scalability as well as online learning agility collectively. The AMTEA lacks scalability due to its computationally intensive EM-based knowledge extraction module whereas the MAB-AMTEA’s source selection strategy, based on the EXP3, struggles to identify related sources quickly and utilize them accordingly. Lastly, we present the trajectory of the learned transfer coefficients of AMTEA and sTrEvo (aggregated per source knapsack type) in Figure 2. As can be seen from Figures 2a to 2d, sTrEvo is able to learn qualitatively similar trends of transfer coefficient values as AMTEA. (Recall that AMTEA is provably optimal whereas sTrEvo follows a randomized (1+1)-ES procedure.) The results show that despite

²Note that the rationale behind proposing MAB-AMTEA in [28] was to tackle the scaling burden of AMTEA when exposed to big task instances.

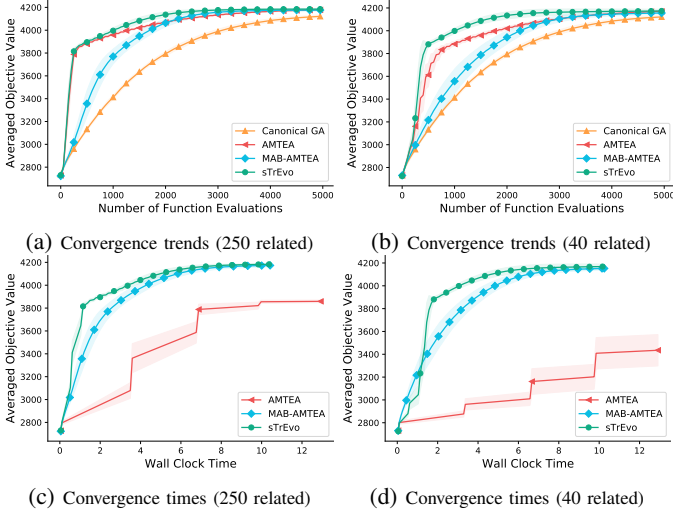


Fig. 1: Averaged performance results of sTrEvo over 30 independent runs for the 0/1 knapsack problem with 1000 source instances. The target is “KP_uc_ac” and the source types are “KP_uc_rc”, “KP_wc_rc”, “KP_sc_rc” and “KP_sc_ac”. Convergence trends relative to the number of function evaluations for (a) 250 related sources and (b) 40 related sources. Convergence trends relative to sTrEvo’s convergence time for (c) 250 related sources and (d) 40 related sources. The shaded region indicates standard deviations either side of the mean.

compromising on optimality, the sTrEvo achieves comparable performance, while simultaneously achieving significantly lower computational cost.

C. Robotic Arm with Variable Morphology

In this section, we consider a planar robotic arm adopted from [41]. In this setting, there is an arm of length L with d joints as equal as its links. (Here d specifies the dimensionality of the problem.) Each joint can rotate to a maximum angle α_{\max} , encoded in $(0, 1]$, which is the same for all joints. Further, all the links have the identical length (here, L'). The problem objective is to find the angle of each joint of the robot (i.e., $\alpha_1, \dots, \alpha_d$) such that the tip of the arm (i.e., the end-effector) is as close as possible to a predefined target in the plane (see Figure 3a).

We identify a task \mathcal{T} by a particular combination of L and α_{\max} in which a candidate solution is encoded by a vector $\alpha = \alpha_1, \dots, \alpha_d$. The fitness function $f(\alpha, \mathcal{T}_{L, \alpha_{\max}})$ to evaluate the solution α to the task $\mathcal{T}_{L, \alpha_{\max}}$ computes the Euclidean distance from the tip position p_d to the target position T . The p_d can be obtained recursively as follows [41]:

$$M_0 = I, \quad (7)$$

$$M_i = M_{i-1} \cdot \begin{pmatrix} \cos \alpha'_i & -\sin \alpha'_i & 0 & L' \\ \sin \alpha'_i & \cos \alpha'_i & 0 & 0 \\ 0 & 0 & 1 & 0 \\ 0 & 0 & 0 & 1 \end{pmatrix}, \quad (8)$$

$$p_i = M_i \cdot (0, 0, 0, 1)^\top, \quad (9)$$

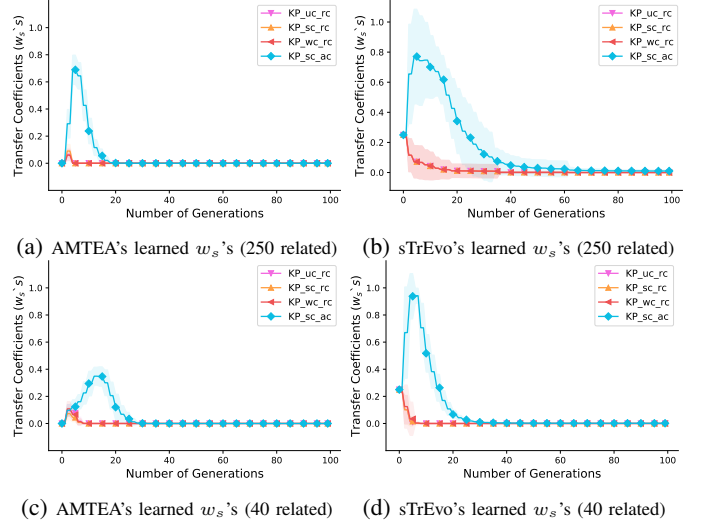


Fig. 2: Learned transfer coefficients of AMTEA and sTrEvo while solving the 0/1 knapsack problem with 1000 sources. (a) AMTEA’s learned w_s ’s with 250 related sources. (b) sTrEvo’s learned w_s ’s with 250 related sources. (c) AMTEA’s learned w_s ’s with 40 related sources. (d) sTrEvo’s learned w_s ’s with 40 related sources. Results were averaged over 30 independent runs. The shaded region indicates standard deviations either side of the mean.

where $\alpha'_i = 2\pi \cdot \alpha_{\max} \cdot (\alpha_i - 0.5)$, $\forall i \in \{1, \dots, d\}$ and $L' = L/d$. Given the above, the fitness function, which calculates the distance between the end of the last link and the target position, can be presented mathematically as,

$$f(\alpha, \mathcal{T}_{L, \alpha_{\max}}) = - \| p_d - T \|. \quad (10)$$

Here, we arbitrary set the target T to $(1, 1)$ in the plane. Note that the objective function is negated in (10) so that the problem can be treated as one of maximization.

We conduct our experimental study for two different scenarios of 10 and 20 joints. The target task is defined as $\mathcal{T}_{\sqrt{2}, 1}$ for both settings, ending up with the largest solution space possible as each joint can rotate from $-\pi$ to π . To identify the sources and their relatedness to the target, we defined 1000 source instances with diverse combinations of L and α_{\max} , ranging between $(0, \sqrt{2})$ and $(0, 1]$, respectively. A continuous CGA was first configured to construct the probabilistic model of one of the sources to optimality. Thereafter, the AMTEA was utilized repeatedly to build the optimized probabilistic models of remaining sources by exploiting the already solved ones. We then sampled 100 solutions from each source model and evaluated them using the objective function of the target task. The average objective value to each source forms a cell of a heatmap, as shown in Figures 3b and 3c for 10 and 20 joints, respectively. Here, the hotter cells indicate more relatedness to the target (as their corresponding mean fitness values are greater) whereas the colder ones show less or no relatedness. Having identified how source-target relatedness is shaped for each scenario, we randomly chose 15 instances with $0 < L < \sqrt{2}$ and $\alpha_{\max} = 1$ as *related* and 985 ones with $0 < L < \sqrt{2}$ and $0.18 < \alpha_{\max} < 0.26$ as *unrelated* to form

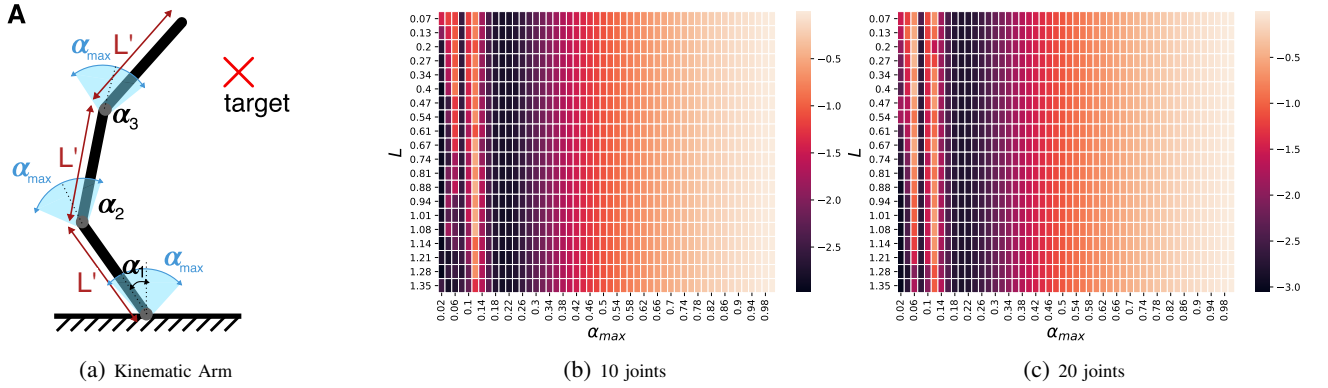


Fig. 3: (a) A planar robotic arm with three joints (and equal links) [41]. The objective is to find the angle of each joint (here, $\alpha_1, \alpha_2, \alpha_3$) such that the end-effector is as close as possible to a predefined target in the plane. Heatmaps of source-target relatedness for diverse combinations of L and α_{\max} , ranging between $(0, \sqrt{2})$ and $(0, 1]$, respectively, for (b) 10 joints and (c) 20 joints. According to the sidebar on the right which marks the fitness range, the hotter cells indicate more relatedness to the target (as their corresponding mean fitness values are greater) whereas the colder ones show less or no relatedness.

a total of 1000 sources per scenario. We followed the same procedure, as already outlined above, to build the probabilistic models of the sources to optimality.

Given that the knowledge extraction module described in Procedure 1 is for the case of a maximization problem, we need some refinements to apply the algorithm for the examples whose underlying optimization problem is one of minimization and $-f_T(\mathbf{x})$ is alternatively being used. The first amendment is on the initial values of the mutation vector. Rather than setting all the values to zeroes, we initialize the mutation vector with a *lower bound* on the fitness value of the target problem. For the robotic arm case study, this was set to the fitness value of the worst feasible solution to the target, which is $-2\sqrt{2}$ when the tip of the arm falls in the opposite direction to the target position. Such adjustment led to more effective exploitation of related sources as demonstrated from our preliminary experiments. The second amendment is to shift the values of the mutation vector to the range $[0, +\infty)$ before applying the maximum absolute scaling function in Line 13 in Procedure 1. This is done by adding all entries by the absolute value of their minimum.

The performance of the sTrEvo was compared with sNES and xNES, as algorithms without transfer capability, in addition to AMTEA and MAB-AMTEA for both 10- and 20-joint evaluation scenarios. A penalty function is embedded in all the compared algorithms to penalize those solutions that violate the α_{\max} constraint. The averaged results obtained over 30 independent runs are shown in Figure 4. With respect to the convergence efficiency, Figures 4a and 4b present the convergence trends of the compared algorithms for 10 and 20 joints, respectively. Both plots strongly advocate the advantage of knowledge transfer not only at reaching the optimality but also at improving the optimization efficiency. Aside from that, we can notice a small spike in averaged objective values in early function evaluations of sTrEvo, further validating our previous findings on the online learning agility of its nested (1+1)-ES when the percentage of related sources is considerably small. Similar to the previous case study, we

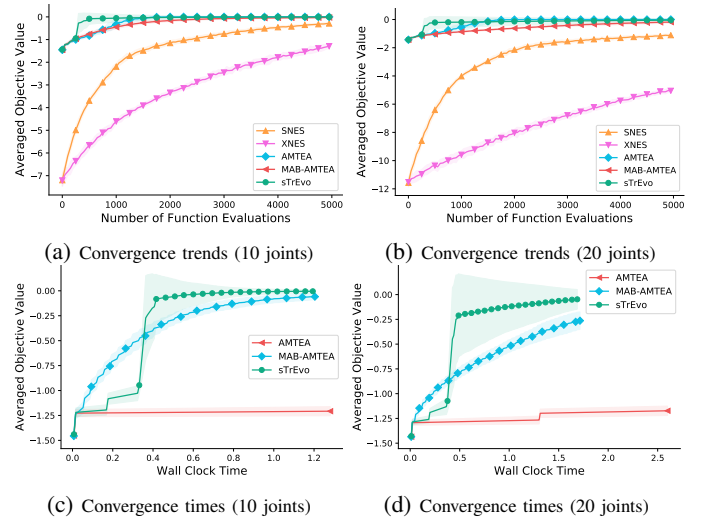


Fig. 4: Averaged performance results of sTrEvo over 30 independent runs for the robotic arm example. The target task is $\mathcal{T}_{\sqrt{2}, 1}$. There are 1000 source instances, 15 of which are related and the rest are unrelated. Convergence trends relative to the number of function evaluations for (a) 10 joints and (b) 20 joints. Convergence trends relative to sTrEvo’s convergence time for (c) 10 joints and (d) 20 joints. The shaded region indicates standard deviations either side of the mean.

also scrutinized the scalability of the sTrEvo against AMTEA and MAB-AMTEA by plotting the convergence trend of the three algorithms within the convergence time of sTrEvo, as shown in Figures 4c and 4d for 10 and 20 joints, respectively. Interestingly, while consistent results can be observed with regard to the computational efficiency of sTrEvo, as elaborated in the previous section, the MAB-AMTEA fails at establishing optimality for the more complex scenario of 20 joints. This indicates that the learning mechanism of the bandit-based approach at choosing only one source each time knowledge transfer occurs is unable to effectively capture related sources to ensure solution optimality.

D. Double Pole Balancing Controller System

Double pole balancing is a prototypical control problem commonly used as a case study for neuro-evolutionary and reinforcement learning algorithms. In this setting, two poles are hinged at the same point to a wheeled cart on a finite length track. The goal is to keep both poles balanced indefinitely by applying a force to the cart at regular intervals without causing the cart to move beyond the track boundaries. The task is more difficult than the basic single pole problem due to nonlinear interactions incurred between the two poles [42].

Six variables are defined to represent the state of the system: the angle of each pole from vertical, the angular velocity of each pole, the position of the wheeled cart on the track, and the velocity of the cart [43]. Regarding the length of the two poles, the long one is fixed to 1 meter whereas the short one is variable (denoted by l) and indicates a task e_l under evaluation. The system is simulated according to the steps instructed in [27]. In this setting, a feedforward neural network (FNN), whose structure remains fixed during the simulation, is used to output a force to the wheeled cart periodically. The conditions for the system failure are either the cart goes out of the track boundaries or one of the two poles loses its balance and drops beyond a certain degree from the vertical. Here, a candidate chromosome represents the connection weights of neurons of the FNN controller and is assessed by measuring the number of time steps elapsed before the system fails. Clearly, the solution quality (fitness) is higher for longer time steps. We assert that a task is solved if a solution could be found such that its corresponding fitness is greater than a specified number of time steps. Following [27], this value was set to 100,000 time steps in our experiments, which is over 30 minutes in simulated time. The architecture of the FNN controller is identical to one applied in [27], i.e., a two-layer network with ten hidden neurons and no bias parameters. This forms a total of 70 weights encoded in the solution chromosome of the evolutionary optimizer.

An established fact concerning the double pole system is that the problem becomes harder to solve when the two poles are very close in length (here, l , the length of the shorter pole, approaches 1m, which is the length of the longer pole). Previous studies suggest incremental learning techniques in which the length of the shorter pole is increased very gradually and then the resultant problem is solved incrementally [43]. The analogy between such incremental problem solving and transfer optimization paradigm was realized in [27] to successfully apply the AMTEA to solve more difficult variants of the problem by utilizing the solutions to easier solved ones. Accordingly, we consider this practical problem as our third case study in this paper to assess how effective and efficient our proposed sTrEvo is at solving increasingly intractable variants of this problem. In this regard, we aim at tackling $e_{0.825}$ as the target problem by building up source problem instances with an ascending order of difficulty starting from $e_{0.1}$ through $e_{0.775}$.

To construct the optimized probabilistic models of the sources, we first configured a continuous GA to solve $e_{0.1}$ to optimality. Thereafter, the AMTEA was applied to solve

TABLE II: Performance comparison of sTrEvo against sNES, xNES, AMTEA and MAB-AMTEA for the double pole balancing problem with $l = 0.825$.

Methods	Successes	Function Evaluations
sNES	0/50	NA
xNES	0/50	NA
AMTEA	34/50	3739 \pm 939
MAB-AMTEA	7/50	4156 \pm 972
sTrEvo	35/50	3108 \pm 993

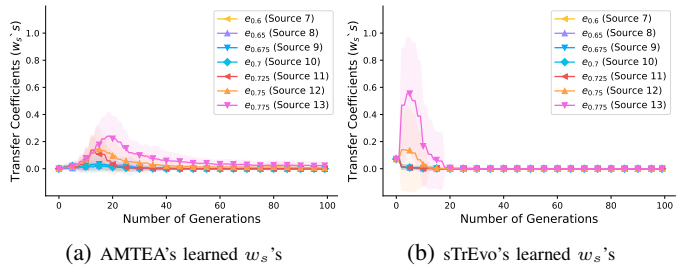


Fig. 5: Learned transfer coefficients of (a) AMTEA and (b) sTrEvo while solving $e_{0.825}$ for the double pole balancing problem. Results were averaged over the corresponding successful runs. The shaded region indicates standard deviations either side of the mean.

the next instances in ascending order of l by utilizing the previously solved ones as the corresponding sources. Following [27], we adopt *success rate* as the performance metric for our experimental study. It is measured by counting the number of runs that each approach is able to solve the problem relative to the total number of runs. We compared sTrEvo with sNES, xNES, AMTEA and MAB-AMTEA by launching each for 50 independent runs. Table II shows the success rate as well as the number of function evaluations averaged over successful runs for the compared algorithms. According to the table, neither sNES nor xNES are able to achieve success in any of their 50 independent runs, revealing the inherent difficulty of $e_{0.825}$. Conversely, both AMTEA and sTrEvo can achieve significantly higher success rates but with noticeably different number of function evaluations, with that of sTrEvo being fewer. The MAB-AMTEA, on the other hand, succeeded for only 7 runs, requiring a considerably higher number of evaluations than AMTEA and, in particular, sTrEvo. Such notable performance of the sTrEvo is mainly due to the online learning agility of its knowledge extraction module, which was also showcased for the other two case studies. Lastly, we present the learned transfer coefficients of AMTEA and sTrEvo averaged over their successful runs for the seven mostly related sources in Figures 5a and 5b, respectively. By observing the two trajectories, we can conclude that sTrEvo is able to learn qualitatively similar trends of transfer coefficient values as the AMTEA but with significantly lower computational cost.

V. CONCLUSION

This paper proposed a novel approach for scalable transfer evolutionary optimization, overcoming two critical shortcomings of today's transfer evolutionary frameworks – namely,

lack of *scalability* when faced with a growing bulk of source problem instances, and lack of *online learning agility* against sparsity of relevant sources to the target task of interest. While applications of existing algorithms are limited to tens of source tasks, in this paper, we took a quantum leap forward in enabling two orders of magnitude scale-up in the number of tasks by handling scenarios with up to thousands of source instances. We devised a scalable transfer evolutionary optimization framework, under the label of sTrEvo, which comprises two co-evolving species for joint evolutions in the space of source knowledge and in the search space of solutions to the target problem. We were able to empirically verify the efficacy of sTrEvo from two aspects of scalability and online learning agility across a set of practically motivated discrete and continuous optimization examples. Such notable performance arises due to,

- 1) the scalability of the (1+1)-ES algorithm nested in sTrEvo with the number of source instances, as only one individual evolves per generation and mutation is the sole reproduction operation;
- 2) the novel mutation mechanism employed in the (1+1)-ES that quickly captures source-target similarities during the course of optimization. This is realized by estimating the expected fitness of source probabilistic models relative to the target objective function, enabling their exploration and exploitation;
- 3) the proposed neutralization strategy in the (1+1)-ES that effectively filters out unrelated sources.

Notably, estimating the expected fitness of each source probabilistic model relative to the target objective function enables source-target similarity matching to be carried out in an offline mode (as was done for the robotic arm example to construct the similarity heatmaps) given a unified search space and known target objective function.

As future work, we plan to generalize sTrEvo to a wider variety of real-world optimization problems characterized by different solution representations; e.g., graph-based representations, scheduling problems, etc. In all such cases, sTrEvo would be designed to be immersed in and leverage big data environments with huge databases of previous optimization experiences. We will also investigate the extensibility of our proposed transfer optimization framework to support *evolutionary multitasking* where mutual exchange of knowledge takes place among multiple optimization problems that are being solved simultaneously within a single population of evolving individuals [44], [45]. In this setting, the reuse of relevant knowledge from past problem-solving instances can be realized across multiple evolving target tasks of interest.

REFERENCES

- [1] Y.-S. Ong and A. Gupta, "Air 5: Five pillars of artificial intelligence research," *IEEE Transactions on Emerging Topics in Computational Intelligence*, vol. 3, no. 5, pp. 411–415, 2019.
- [2] A. Gupta, Y.-S. Ong, and L. Feng, "Insights on transfer optimization: Because experience is the best teacher," *IEEE Transactions on Emerging Topics in Computational Intelligence*, vol. 2, no. 1, pp. 51–64, 2017.
- [3] A. Gupta and Y.-S. Ong, *Memetic Computation: The Mainspring of Knowledge Transfer in a Data-Driven Optimization Era*. Springer, 2018, vol. 21.
- [4] A. T. W. Min, Y.-S. Ong, A. Gupta, and C.-K. Goh, "Multiproblem surrogates: Transfer evolutionary multiobjective optimization of computationally expensive problems," *IEEE Transactions on Evolutionary Computation*, vol. 23, no. 1, pp. 15–28, 2017.
- [5] L. Feng, Y.-S. Ong, S. Jiang, and A. Gupta, "Autoencoding evolutionary search with learning across heterogeneous problems," *IEEE Transactions on Evolutionary Computation*, vol. 21, no. 5, pp. 760–772, 2017.
- [6] J. Zhang, W. Zhou, X. Chen, W. Yao, and L. Cao, "Multi-source selective transfer framework in multi-objective optimization problems," *IEEE Transactions on Evolutionary Computation*, 2019.
- [7] L. Feng, Y.-S. Ong, M.-H. Lim, and I. W. Tsang, "Memetic search with interdomain learning: A realization between cvrp and carp," *IEEE Transactions on Evolutionary Computation*, vol. 19, no. 5, pp. 644–658, 2014.
- [8] L. Feng, Y.-S. Ong, A.-H. Tan, and I. W. Tsang, "Memes as building blocks: a case study on evolutionary optimization+ transfer learning for routing problems," *Memetic Computing*, vol. 7, no. 3, pp. 159–180, 2015.
- [9] M. A. Ardeh, Y. Mei, and M. Zhang, "A novel genetic programming algorithm with knowledge transfer for uncertain capacitated arc routing problem," in *Pacific Rim International Conference on Artificial Intelligence*. Springer, 2019, pp. 196–200.
- [10] R. Lim, Y.-S. Ong, H. T. H. Phan, A. Gupta, and A. N. Zhang, "Can route planning be smarter with transfer optimization?" in *Proceedings of the Genetic and Evolutionary Computation Conference Companion*, 2019, pp. 318–319.
- [11] M. Jiang, Z. Huang, L. Qiu, W. Huang, and G. G. Yen, "Transfer learning-based dynamic multiobjective optimization algorithms," *IEEE Transactions on Evolutionary Computation*, vol. 22, no. 4, pp. 501–514, 2017.
- [12] X.-F. Liu, Z.-H. Zhan, T.-L. Gu, S. Kwong, Z. Lu, H. B.-L. Duh, and J. Zhang, "Neural network-based information transfer for dynamic optimization," *IEEE transactions on neural networks and learning systems*, 2019.
- [13] M. Jiang, Z. Wang, S. Guo, X. Gao, and K. C. Tan, "Individual-based transfer learning for dynamic multiobjective optimization," *IEEE Transactions on Cybernetics*, 2020.
- [14] M. Iqbal, W. N. Browne, and M. Zhang, "Extracting and using building blocks of knowledge in learning classifier systems," in *Proceedings of the 14th annual conference on Genetic and evolutionary computation*, 2012, pp. 863–870.
- [15] —, "Reusing building blocks of extracted knowledge to solve complex, large-scale boolean problems," *IEEE Transactions on Evolutionary Computation*, vol. 18, no. 4, pp. 465–480, 2013.
- [16] M. Iqbal, B. Xue, H. Al-Sahaf, and M. Zhang, "Cross-domain reuse of extracted knowledge in genetic programming for image classification," *IEEE Transactions on Evolutionary Computation*, vol. 21, no. 4, pp. 569–587, 2017.
- [17] A. T. W. Min, R. Sagarna, A. Gupta, Y.-S. Ong, and C. K. Goh, "Knowledge transfer through machine learning in aircraft design," *IEEE Computational Intelligence Magazine*, vol. 12, no. 4, pp. 48–60, 2017.
- [18] L. Feng, Y. Huang, I. W. Tsang, A. Gupta, K. Tang, K. C. Tan, and Y.-S. Ong, "Towards faster vehicle routing by transferring knowledge from customer representation," *IEEE Transactions on Intelligent Transportation Systems*, 2020.
- [19] A. T. W. Min, A. Gupta, and Y.-S. Ong, "Generalizing transfer bayesian optimization to source-target heterogeneity," *IEEE Transactions on Automation Science and Engineering*, 2020.
- [20] T. T. Joy, S. Rana, S. Gupta, and S. Venkatesh, "A flexible transfer learning framework for bayesian optimization with convergence guarantee," *Expert Systems with Applications*, vol. 115, pp. 656–672, 2019.
- [21] T. G. Karimpanal, S. Rana, S. Gupta, T. Tran, and S. Venkatesh, "Learning transferable domain priors for safe exploration in reinforcement learning," in *2020 International Joint Conference on Neural Networks (IJCNN)*. IEEE, 2020, pp. 1–10.
- [22] S. J. Louis and J. McDonnell, "Learning with case-injected genetic algorithms," *IEEE Transactions on Evolutionary Computation*, vol. 8, no. 4, pp. 316–328, 2004.
- [23] P. Cunningham and B. Smyth, "Case-based reasoning in scheduling: reusing solution components," *International Journal of Production Research*, vol. 35, no. 11, pp. 2947–2962, 1997.
- [24] M. Kaedi and N. Ghasem-Aghaee, "Biasing bayesian optimization algorithm using case based reasoning," *Knowledge-Based Systems*, vol. 24, no. 8, pp. 1245–1253, 2011.
- [25] S. Didi and G. Nitschke, "Multi-agent behavior-based policy transfer," in *European Conference on the Applications of Evolutionary Computation*. Springer, 2016, pp. 181–197.

- [26] S. Friess, P. Tiño, S. Menzel, B. Sendhoff, and X. Yao, “Improving sampling in evolution strategies through mixture-based distributions built from past problem instances,” in *International Conference on Parallel Problem Solving from Nature*. Springer, 2020, pp. 583–596.
- [27] B. Da, A. Gupta, and Y.-S. Ong, “Curbing negative influences online for seamless transfer evolutionary optimization,” *IEEE transactions on cybernetics*, vol. 49, no. 12, pp. 4365–4378, 2019.
- [28] M. Shakeri, A. Gupta, Y.-S. Ong, X. Chi, and A. Z. NengSheng, “Coping with big data in transfer optimization,” in *2019 IEEE International Conference on Big Data (Big Data)*. IEEE, 2019, pp. 3925–3932.
- [29] L. Feng, L. Zhou, J. Zhong, A. Gupta, Y.-S. Ong, K.-C. Tan, and A. K. Qin, “Evolutionary multitasking via explicit autoencoding,” *IEEE transactions on cybernetics*, vol. 49, no. 9, pp. 3457–3470, 2019.
- [30] P. Smyth and D. Wolpert, “Stacked density estimation,” in *Advances in neural information processing systems*, 1998, pp. 668–674.
- [31] T. K. Moon, “The expectation-maximization algorithm,” *IEEE Signal processing magazine*, vol. 13, no. 6, pp. 47–60, 1996.
- [32] P. Auer, N. Cesa-Bianchi, Y. Freund, and R. E. Schapire, “Gambling in a rigged casino: The adversarial multi-armed bandit problem,” in *Proceedings of IEEE 36th Annual Foundations of Computer Science*. IEEE, 1995, pp. 322–331.
- [33] —, “The nonstochastic multiarmed bandit problem,” *SIAM journal on computing*, vol. 32, no. 1, pp. 48–77, 2002.
- [34] D. Wierstra, T. Schaul, T. Glasmachers, Y. Sun, J. Peters, and J. Schmidhuber, “Natural evolution strategies,” *The Journal of Machine Learning Research*, vol. 15, no. 1, pp. 949–980, 2014.
- [35] H. Mühlenbein, “The equation for response to selection and its use for prediction,” *Evolutionary Computation*, vol. 5, no. 3, pp. 303–346, 1997.
- [36] K. Deb, R. B. Agrawal *et al.*, “Simulated binary crossover for continuous search space,” *Complex systems*, vol. 9, no. 2, pp. 115–148, 1995.
- [37] K. Deb and D. Deb, “Analysing mutation schemes for real-parameter genetic algorithms,” *International Journal of Artificial Intelligence and Soft Computing*, vol. 4, no. 1, pp. 1–28, 2014.
- [38] C. B. Do, “The multivariate gaussian distribution,” 2008.
- [39] T. Schaul, J. Bayer, D. Wierstra, Y. Sun, M. Felder, F. Sehnke, T. Rückstieß, and J. Schmidhuber, “PyBrain,” *Journal of Machine Learning Research*, vol. 11, pp. 743–746, 2010.
- [40] Z. Michalewicz and J. Arabas, “Genetic algorithms for the 0/1 knapsack problem,” in *International Symposium on Methodologies for Intelligent Systems*. Springer, 1994, pp. 134–143.
- [41] J.-B. Mouret and G. Maguire, “Quality diversity for multi-task optimization,” *arXiv preprint arXiv:2003.04407*, 2020.
- [42] F. Gomez, J. Schmidhuber, and R. Miikkulainen, “Accelerated neural evolution through cooperatively coevolved synapses,” *Journal of Machine Learning Research*, vol. 9, no. May, pp. 937–965, 2008.
- [43] F. J. Gomez and R. Miikkulainen, “Solving non-markovian control tasks with neuroevolution,” in *IJCAI*, vol. 99, 1999, pp. 1356–1361.
- [44] Y.-S. Ong and A. Gupta, “Evolutionary multitasking: a computer science view of cognitive multitasking,” *Cognitive Computation*, vol. 8, no. 2, pp. 125–142, 2016.
- [45] K. K. Bali, A. Gupta, Y.-S. Ong, and P. S. Tan, “Cognizant multitasking in multiobjective multifactorial evolution: Mo-mfea-ii,” *IEEE Transactions on Cybernetics*, 2020.